Environ. Eng. Res. Vol. 9, No. 5, pp. 201~213, 2004
Korean Society of Environmental Engineers

EFFECT OF DENSITY FLOW REGIMES ON THE FATE OF A TOXIC SUBSTANCE IN A STRATIFIED RESERVOIR

Se-Woong Chung†

Department of Environmental Eng., Chungbuk National University, Cheongju 361-763, Korea

(received July 2004, accepted September 2004)

Abstract : The transport and fate of toxic chemicals in a stratified reservoir are closely related to density flow regimes in the reservoir. To better understand the behavior of toxic substances under reservoir stratification, a two-dimensional toxic model was developed and incorporated into the laterally integrated hydrodynamics and transport model, CE-QUAL-W2. To validate the model, it was applied to Shasta Reservoir, California where a spill of volatile toxic compound, methyl isothiocyanate (MITC) had happened and field data were secured during the spill. The predicted MITC concentrations were compared with that observed. The model showed a great performance in replicating the density flow regimes and fate of the MITC plume. The model was applied to identify the effect of two different density flow regimes, interflow and overflow on the degradation of MITC. The persistence of MITC was significantly influenced by different flow regimes. MITC was more persistent in the reservoir under interflow regime due to reduced volatilization from deep layers than under overflow condition. In the overflow situation, the plume moved more slowly toward dam and experienced greater degradation. The model can be effectively used to assist in making a contingent plan from toxicant spill, which may happen by accident or military purposes.

Key Words : Toxic model, density flow regimes, CE-QUAL-W2, reservoir, contingent plan

INTRODUCTION

Toxic substance spill, which might happen by accidents, heavy storm events or military purposes, into rivers and reservoirs can severely affect fisheries and local water supply systems in a short time period.[1,2] The environmental and economic impacts of a chemical spill into a reservoir can be fatal for a community, in particular, if the community is heavily rely on the reservoir for water supply. In the Midwestern United States reservoirs, frequent occurrence of high levels of pesticides during late spring and early summer is one of the most serious water quality issues.[3] The levels of some pesticides occasionally exceeded their maximum contamination levels (MCL) for drinking water with potential adverse impacts on human health.[4,5] Therefore, a full understanding of the transport and fate of toxic substances in a reservoir during a spill or peak runoff loading period is essential in establishing an effective management strategy and protecting the scarce water resources.

Once a toxic chemical enters a reservoir, its fate and transport are governed by various factors including reservoir hydrodynamics, chemical and biological conditions of the waterbody, weather factors, and properties of the toxicant. The processes can be furthermore complicated if the reservoir is stratified and a

† Corresponding author
E-mail: schung@chungbuk.ac.kr
Tel: 043-261-3370, Fax: 043-272-3370

density flow forms due to the temperature difference between river and ambient waters. The kinetic (decay) processes can be largely influenced by flow regimes, i.e., overflow, plunge flow, underflow, and interflow.[6] Some chemicals are potentially more degradable through volatilization, photolysis, and oxidation because sufficient turbulence, sunlight, and oxygen are available near the water surface if the inflow becomes an overflow. Therefore, a water quality model should adequately link the kinetic processes with reservoir hydrodynamics for better prediction of the persistence and spatial distribution of the toxicant during a spill or runoff.

A laterally integrated two-dimensional (2D) hydrodynamics and transport model, CE-QUAL-W2[7] has been broadly used for the modeling of water temperature and conventional water quality constituents in reservoirs.[8-12] However, its application has been limited to conventional constituents by the lack of a toxic simulation model. The objectives of this study are to develop a toxic module for CE-QUAL-W2, test the model against field data, and investigate the effect of reservoir flow regimes on the fate and transport of a volatile toxic compound in a stratified reservoir during a spill event. The model was validated against filed data collected from the Shasta Reservoir, California, during the 1991 spill. Observed and simulated chemical concentrations were used to analyze the fate and transport processes of the spilled chemical, methyl isothiocyanate (MITC). The effect of two different flow regimes, interflow and overflow, on the degradation of MITC was examined by simulations.

MODEL DEVELOPMENT

Governing Equations

Toxic substances may decay in the adsorbed particulate form, but decay was assumed to occur only in the dissolved phase to simplify the processes.[13] A linear sorption-desorption kinetics was adopted because chemical concentrations in water column are mostly environmentally relevant, i.e., less than one-half water solubility. An instantaneous local equilibrium was assumed for sorption process since the time scale for sorption reactions is much smaller than that of other kinetic and macroscopic transport (advection and dispersion) processes in reservoirs.

By the law of mass conservation, the governing equations for total chemical concentrations in water column ($C_{t,w}$) and bed sediments ($C_{t,b}$) are formulated as (1) and (2), respectively.

$$\frac{\partial(BC_{t,w})}{B\partial t}+\frac{\partial(UBC_{t,w})}{B\partial x}+\frac{\partial(WBC_{t,w})}{B\partial z}-\frac{\partial}{B\partial x}(BD_x\frac{\partial C_{t,w}}{\partial x})-\frac{\partial}{B\partial z}(BD_z\frac{\partial C_{t,w}}{\partial z})$$
$$=\frac{K_f}{y}(f_{d,b}C_{t,b}/\phi-f_{d,w}C_{t,w})-(K_P+K_H+K_O+K_B)f_{d,w}C_{t,w}$$
$$+\frac{k_l}{z}\{(C_a/H)-f_{d,w}C_{t,w}\}-\frac{v_s}{z}f_{p,w}C_{t,w}+\Phi_{NPS} \quad (1)$$

$$\frac{\partial(BC_{t,b})}{B\partial t}=-\frac{K_f}{y}(f_{d,b}C_{t,b}/\phi-f_{d,w}C_{t,w})-(K_H+K_O+K_B)f_{d,b}C_{t,b}$$
$$+\frac{v_s}{z}f_{p,w}C_{t,w} \quad (2)$$

where, subscripts t, d and p denote the total, dissolved, and particulate phases of a chemical, respectively; subscripts a, w and b denote air, water, and bed, respectively; f_d and f_p are the fractions of dissolved and particulate chemicals to the total chemical; t is time; x is longitudinal Cartesian coordinate (positive to the right); B is waterbody width; U and W are longitudinal and vertical flow velocities; D_x and D_z are longitudinal and vertical constituent dispersion coefficients, respectively; K_f is diffusive exchange rate between water column and pore water of the bed; ϕ is the porosity of the bed sediments; K_P, K_H, K_O, and K_B are rate constants for photolysis, hydrolysis, oxidation, and biotransformation, respectively; k_l is air-water exchange rate due to volatilization; H is Henry's constant; C_a is vapor phase concentration; Φ_{NPS} is the nonpoint source (NPS) mass flow rate per unit volume; v_s is the net settling velocity of sorbed chemical; z is the depth of water from water surface; and y is the distance from reservoir

bottom. The chemical kinetic reaction rates and model input parameters can be determined from field and laboratory experiments, estimation using chemical properties, and previous literature.[14-15]

Transport of sediments in water column and reservoir bed was formulated using the 2D laterally integrated advection-dispersion equations, assuming a stationary bed condition as equations (3) and (4).

$$\frac{\partial(BC_s)}{B\partial t}+\frac{\partial(UBC_s)}{B\partial x}+\frac{\partial(WBC_s)}{B\partial z}-\frac{\partial}{B\partial x}(BD_x\frac{\partial C_s}{\partial x})-\frac{\partial}{B\partial z}(BD_z\frac{\partial C_s}{\partial z})= -\frac{v_{ss}}{\Delta z}C_{ss}-K_{dt}\gamma_{om}C_{dt}-\frac{v_{dt}}{\Delta z}C_{dt}+q_l \quad (3)$$

$$\frac{\partial(BC_b)}{B\partial t}=\frac{v_s}{\Delta z}C_{ss}+\frac{v_{dt}}{\Delta z}C_{dt}-\gamma_{om}K_sC_b+q_b \quad (4)$$

where, C_s is sediments concentration including inorganic and organic (detritus) sediments in water column; q_l is lateral mass flow rate of sediments per unit volume for water column; v_{ss} is net settling velocity of suspended solids; C_{ss} is suspended solids concentration; (z is cell thickness; K_{dt} is detritus decay rate; v_{dt} is net detritus settling rate; and C_{dt} is detritus concentration in water column; C_b is the total bed sediment concentration; γ_{om} is rate multiplier for temperature adjustment; K_s is organic bed sediment decay rate; and q_b is lateral mass flow rate of sediments per unit volume for bed sediments.

Physical, Chemical and Biological Processes

A partition coefficient (K) was used to determine the fractions of dissolved and particulate chemical forms to the total chemical based on the linear sorption-desorption kinetics. For the equilibrium phase partitioning, two phases and particle interaction models were adopted.[16-17] Dissolved chemical in water column may transfer to interstitial water in the bottom sediment by diffusion process in the initial stages of a chemical spill, or vice verse may occur during the recovery phase depending on the concentration gradient. This mass-transfer was estimated as a function of molecular weight (M) of a chemical and porosity of bed sediments[18] as follows:

$$K_f = 19\phi(M)^{\frac{-2}{3}} \quad (5)$$

The amount of chemical loss due to photolysis is a function of the quantity and wavelength distribution of incident light, the light absorption characteristics of the chemical, and the efficiency at which absorbed light yields a chemical reaction. A first-order reaction constant was used to estimate the rate of photolysis[19]:

$$K_p = K_{do}\frac{I_o}{I_o'}\frac{D}{D_o}\left\{\frac{1-\exp[-K_e(\lambda_{max})\cdot z]}{K_e(\lambda_{max})\cdot z}\right\} \quad (6)$$

where K_{do} is the direct near surface photolysis rate; I_o is the daily amount of incoming solar radiation at the water surface; Io' is the light intensity at which K_{do} was measured; D is the radiance distribution function; D_o is the radiance distribution function near the surface; and K_e (λ_{max}) is the net light extinction coefficient at λ_{max}, the wavelength of the maximum light absorption. Extinction coefficients for water, inorganic, and organic sediments were used to calculate a net light extinction coefficient, K_e.

Hydrolysis is a major decay process in which a chemical compound reacts with water molecules and results in a cleavage of a chemical bond. Generally, hydrolysis is a second-order reaction because of dependence on the molar concentrations of $[H^+]$, $[OH^-]$, or water mediators. A pseudo-first-order rate constant $K_H = K_n + K_a[H^+] + K_b[OH^-]$ was used, where K_n is the neutral hydrolysis rate, K_a is the acid catalyzed hydrolysis rate, and K_b is the base catalyzed hydrolysis rate. Arrhenius function was used to adjust the rate with temperature.

Toxic chemicals can be oxidized by a reaction with either dissolved oxygen or free radicals in natural waters. A pseudo-first-order reaction rate constant was used to compute

degradation of a chemical by oxidation assuming that the rate of free radical formation (oxidant) is relatively constant (steady state). The rate was adjusted using Arrhenius function depending on water temperature.

Biotransformation is the microbially mediated decay processes by which a chemical is degraded by bacteria and fungi. The model was designed to treat the biotransformation process either by second-order or pseudo-first-order reactions based on the Monod equation:

$$\frac{dC_d}{dt} = -\frac{1}{y_B}\frac{dC_B}{dt} = \frac{\mu_{\max}}{y_B}\left(\frac{C_d}{K_s + C_d}\right)C_B \quad (7)$$

where C_B is the bacterial concentration; y_B is the bacterial yield coefficient; $\mu_{\max}$ is the maximum specific growth rate; and K_s is the half-saturation constant. The rate was adjusted with water temperature.

A modified two-film theory[20,21] was used to compute the gaseous transfer of chemical from air to water and water to air. The transfer rate was proportional to the concentration gradient between the chemicals in water column and in the overlying atmosphere. The overall transfer coefficient, k_l, was given as follows:

$$\frac{1}{k_l} = \frac{1}{K_l} + \frac{1}{K_g H} \quad (8)$$

where K_l is the liquid film coefficient and K_g is the gas film coefficient. The k_l value was computed as a function of the chemical characteristics (H, K_l and K_g), water velocity, and wind speed. Since the transfer coefficient for the open bodies of water such as reservoir and lake are largely affected by wind, O'Connor (1983)[20] and Mackay (1982)[21] equations were incorporated into the model for the estimation of the liquid and gas film transfer coefficients.

Numerical Method and Computer Programming

The governing equations were solved using the finite-difference methods as used in the CE-QUAL-W2. The dependent variables are toxicant and sediment concentrations in the water column and bed sediments. The independent variables are longitudinal distance, flow depth, and time. Figure 1 briefly describes the overall algorithms of the model.

The equations for toxicant and sediment transport were solved using the explicit QUICKEST (Quadratic Upstream Interpolation for Convective Kinematics with Estimated Streaming Terms) finite difference scheme.[22] Vertical turbulent transfer of toxic contaminants was determined from the vertical shear of horizontal velocity and a density gradient dependent Richardson number function. The physical, chemical, and biological properties of a toxic chemical and its kinetic reaction rates need to be provided through an input file. The model can compute kinetic decay processes either independently by providing individual kinetic reaction rates or collectively by providing a lumped value of transformation rate or half-life. Time-variable half-life values can be specified in the model.

MODEL APPLICATION

Spill and Site Descriptions

On July 14, 1991, approximately 49 to 72 thousands liters of VAPAM liquid formulation were estimated to have spilled into the Sacramento River, California (Figure 2).[23,24] VAPAM, sodium methyl dithiocarbamate (Na-MDTC), is a toxic pesticide and decomposes into more stable products, primarily the far more toxic chemical methyl isothiocyanate (MITC, $CH_3N{=}C{=}S$) in water. During traveling the long Sacramento River, which provided good environments such as high level of lights and oxygen for the chemical reactions, Na-MDTC transformed into more toxic MITC through oxidation and photolysis.[25] The LC_{50} (96-h) of MITC, that is the lethal concentration at which 50% mortality occurs from 96 hours exposure time, for bluegill is 130 μg/L[26], indicating the strong toxicity of the chemical. A great number of fish

died during the spill. A large portion of the MITC was vaporized into the air and impaired human health in the vicinity of the spill site. The residual MITC, eventually, entered into the Shasta Reservoir at midnight of July 16.

The reservoir was stratified during the spill period. Temperatures in the reservoir showed that vertical and longitudinal variations were significant, but lateral variations are generally small in the upper reach from the head of the reservoir to its confluence with the Squaw River arm.[27] Water temperatures in the reservoir were in the range of 19 to 27.5°C in the epilimnion and 7 to 16 °C in the hypolimnion. The river flow entering the reservoir averaged 7.5 m^3/s with a temperature of 18-24 °C during the spill. Under these conditions, the contaminated river flow plunged after entering the reservoir and formed an underflow and interflow.[6]

Water sampling and field monitoring were conducted to keep track of the spill after it entered the Shasta Reservoir. The spill managers marked the contaminant plume with the red dye rhodamine WT to track its progress in the reservoir when the plume plunged into the reservoir. An artificial mixing device was

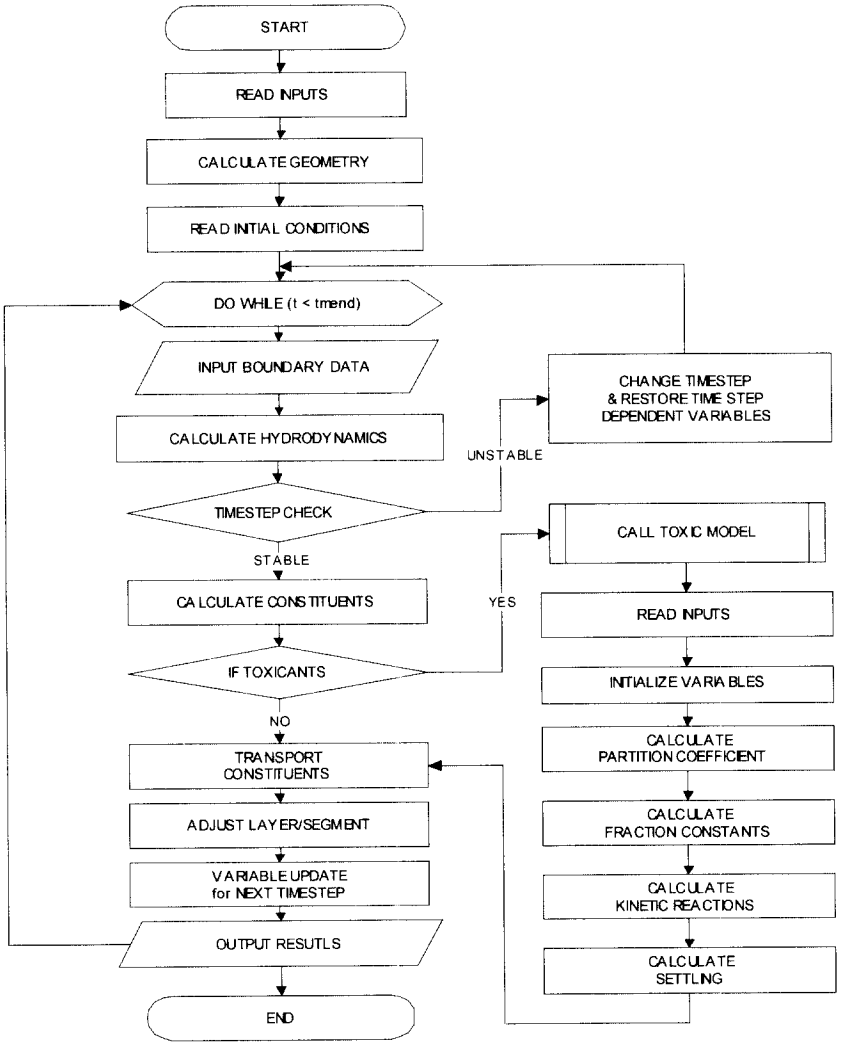

Figure 1. The flowchart of numerical processes of the toxic module in CE-QUAL-W2.

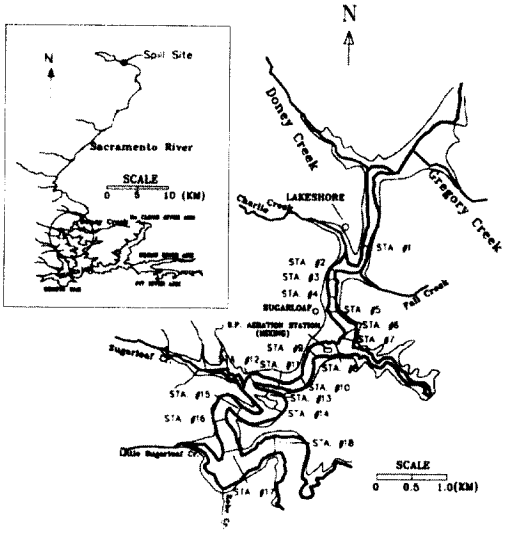

Figure 2. Map of the spill site and sampling stations in the Shasta Reservoir.

installed at the distance of about 2.6 km downstream from the head of reservoir to mix the contaminant plume with the reservoir water.

In this model application, the time-varying MITC boundary concentrations were specified at the upper end of the computational domain, Doney Creek. Data were obtained on an hourly basis from midnight of July 16, 1991 when the plume arrived at Doney Creek, to 10:10 a.m. next day. Only three measurements were taken additionally until noon on July 19. The MITC concentrations varied with time, from 2 mg/L at midnight on July 16 to 35 mg/L (peak) at 5:00 a.m. and 5 mg/L at 10:00 a.m. on July 17, and dropped to a non-detectable level (< 0.001 mg/L) at noon on July 19. The peak concentration (C_o) passed Doney Creek at 5:00 a.m. on July 17. Initial and boundary conditions for flows, temperature, and weather conditions were set based on the observed data.

Computational Domain and Simulation Period

Insignificant lateral variation, small expansion angle, mild bottom slope, and stable stratification make it appropriate to apply the laterally-averaged 2D model to the upper reach of the Shasta Reservoir. A finite difference grid system was generated, consisting of 32 segments with lengths of 200-1000 m in the longitudinal direction and 52 vertical layers with thickness of 0.5-4 m. The nonuniform grid system has finer grids in the plunging region and coarser grids in other regions. Bathymetry data were made using USGS topographic maps. The inflow width and depth at Doney Creek was 70 m and 1.0 m, respectively. July 16 to 24, 1991 was chosen as the simulation period because the field measurements of MITC dropped to a non-detectable level after July 24, 1991. Variable time-steps were used in the simulations, which are a fraction of the maximum time step calculated from the numerical stability criterion with an autostepping algorithm.

Degradation Processes of MITC

The degradation of MITC due to physico-chemical processes is dependent upon the chemical properties and environmental conditions of the reservoir such as the level of turbulence,

Table 1. Physical and chemical properties of methyl isothiocyanate (MITC)

Property	Unit	Value
Molecular weight	g/mol	73
Solubility	mg/L	7600
Vapor pressure at 20 °C	kPa	2.7
Henry's constant	atm-m^3/mol	0.26×10^{-3}
Octanol-water partition K_{ow}	-	23.5
Specific gravity at 20 °C	g/cm^3	1.048
Diffusivity in water[a]	cm^3/s	1.26×10^{-6}
Diffusivity in air[a]	cm^3/s	0.109

[a]Calculated as a function of molecular weight.

temperature, dissolved oxygen, and solar radiation that are all function of water depth in a stratified reservoir. MITC is a volatile compound with high solubility and low adsorption potential in water as shown in Table 1. In general, MITC is known to be volatile and reactive when exposed to elevated temperature, oxygen level, and sunlight. However, its fate in surface waters is not investigated well.[23]

Previous studies concluded that the primary pathways of MITC degradation in surface water are volatilization and hydrolysis.[23,25,27] Direct photolysis rate of MITC in surface water is a function of water depth.[29] Draper and Wakeham (1993)[30] found that MITC is resistant to photodegradation in water. No detectable MITC photolysis occurred after 5 hours of irradiation in laboratory experiments. The sorption of MITC onto suspended solids is negligible in surface water if suspended solids concentration (C_{ss}) is low.[25] The fraction of dissolved MITC, f_d, was estimated as a function of partition coefficient, C_{ss}, and the fraction of organic matter (Figure 3). It was found that more than 97% of MITC was in the dissolved form as the C_{ss} was far below 1000 mg/L during the spill. Therefore, it is assumed in the simulations that MITC degradations were primarily through volatilization and hydrolysis.

The rate of volatilization from water to air was influenced by both chemical properties such as molecular weight, Henry's constant, and environmental conditions at the air-water interface, i.e., turbulence controlled by wind speed and current velocity, and water depth. The hydrolysis of MITC through the reaction with water molecules is a strong function of the pH level of water.[28] The first-order hydrolysis rate constant (K_h) for MITC was obtained from its half life ($t_{1/2}$) value in the neutral water (490 hours at pH = 7) using the relation of $K_h = 0.693/t_{1/2}$.

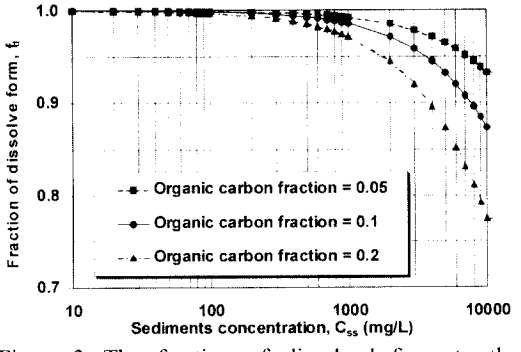

Figure 3. The fraction of dissolved form to the total MITC concentration in water as a function of sediments concentration and fraction of organic carbon.

RESULTS AND DISCUSSION

Fate and Transport of MITC

Simulated MITC concentrations in the reservoir are presented in Figure 4 in the form of iso-concentration contours. The MITC contours are 3, 30, and 60 hours after the peak passed the upstream boundary.

The levels of MITC decay shown in Figure 4b were obtained by subtracting the concentrations of MITC from the concentrations of a tracer (a conservative matter), and are used to determine the effectiveness of the kinetic processes in the total MITC reduction. The chemical decay was greater in the plunge flow and underflow compare to the interflow. This is mainly attributed to the strong turbulence near the surface of the reservoir induced by wind and flow which accelerated volatilization of the contaminant. In the interflow, the strong reservoir stratification limited the gaseous transfer of the contaminant from water to air.

The effectiveness of chemical reactions on the total concentration reduction, E_R, was quantitatively analyzed using the predicted maximum chemical concentrations at different times and in different flow regimes (Table 2). C_{tracer} and C_{mitc} denote the predicted maximum tracer and MITC concentrations in the reservoir after time t (hours), respectively.

The total concentration reduction after time t was obtained by subtracting C_{mitc} from the peak concentration at the inflow boundary, C_o. The total reduction rate (R_T), which was defined by $100 \times (C_o - C_{mitc})/C_o$, increased exponentially with time. More than 80% of concentration reduction

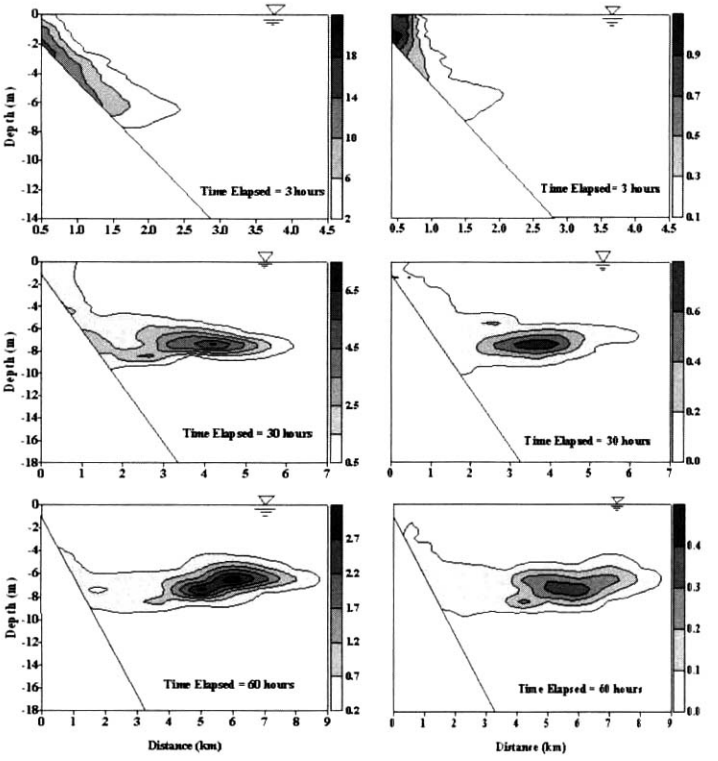

Figure 4. Contours of the simulated MITC concentrations (a) and concentration difference between tracer and MITC (b) that represents the level of decay.

Table 2. The effects of flow dilution and physico-chemical reactions on total MITC reduction versus time in various flow regimes

Time (hours) (1)	Flow regime (2)	C_{tracer} (mg/L) (3)	C_{mitc} (mg/L) (4)	C_o- C_{mitc} (mg/L) (5)	R_T (%) (6)	I_D (%) (7)	I_R (%) (8)	E_R (%) (9)
0	Inflow	35.0	35.0	0.0	0.0	-	-	-
3	Plunge flow	22.9	22.0	13.0	37.1	93.1	6.9	3.9
12	Underflow	9.9	9.1	25.9	74.0	96.9	3.1	8.1
30	Interflow	5.6	5.0	30.0	85.7	98.0	2.0	10.7
57	Interflow	3.4	3.0	32.0	91.4	98.7	1.3	11.8
81	Interflow	2.8	2.4	32.5	92.8	99.1	0.9	14.3

(1) Time elapsed after the peak passed the upstream boundary (Doney Creek).
(2) Reservoir flow regime.
(3) Peak tracer concentration (dilution effect).
(4) Peak MITC concentration (dilution and physico-chemical reactions effect).
(5) Total reduction of peak MITC concentration.
(6) Total MITC reduction rate, $R_T = 100((C_o - C_{mitc})/C_o$
(7) Dilution index, $I_D = 100 \times (C_o - C_{tracer})/(C_o - C_{mitc})$
(8) Reaction index, $I_R = 100 \times (C_{tracer} - C_{mitc})/(C_o - C_{mitc})$
(9) Effectiveness of chemical reactions at time t, $E_R = 100 \times (C_{tracer,t} - C_{mitc,t}) / C_{tracer,t}$

was accomplished within 30 hours after the peak passed the upper boundary of the reservoir. A dilution index (I_D) and a reaction index (I_R) were used to separate the contributions of flow dilution by mixing processes and chemical decay by physical and chemical reaction processes. The I_D and I_R values vary from 0 to 100%, and their sum should be always equal to 100%. An index

value of 100% indicates that the total reduction of chemical concentrations is accomplished by the dilution (I_D = 100%) or reactions (I_R = 100%). Therefore, a large E_R value indicates a great effectiveness of chemical reactions at time t.

The I_R value reached as high as about 7% in the plunge flow region due to the high chemical concentrations and flow turbulence. Although the IR value constantly decreased to 2-3% in the underflow and to less than 1% after 81 hours in the interflow, the E_R value increased with time as the turbulent mixing decreased. The results imply that the reduction of MITC was primarily attained by flow dilution (i.e., I_D > 90%) in the early stage of the spill, but the influence of physical and chemical reaction processes increase with time and can be significant in the late stage of the spill. Thus, it is possible that the persistence of MITC is more likely dependent upon the decay processes rather than the turbulent mixing processes in the late stage.

Observed and simulated MITC concentrations at different stations are presented in Figure 5. The large deviation between observed and simulated concentrations at Station 1 may be attributed to two reasons, i.e., inaccurate prediction of wind mixing effects in the epilimnion due to lack of wind direction data and a continuous break down of small amount of residual Na-MDTC near the reservoir surface. Due to the artificial mixing device that was operated at just upstream of sampling station 9,

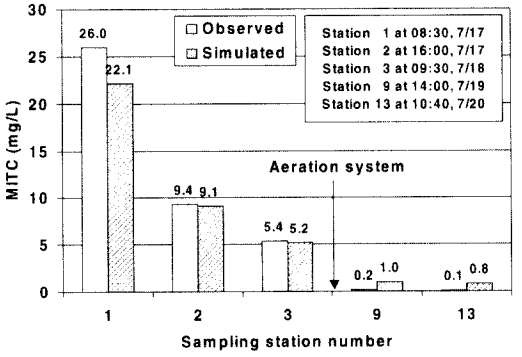

Figure 5. Observed and simulated MITC concentrations at selected sampling stations.

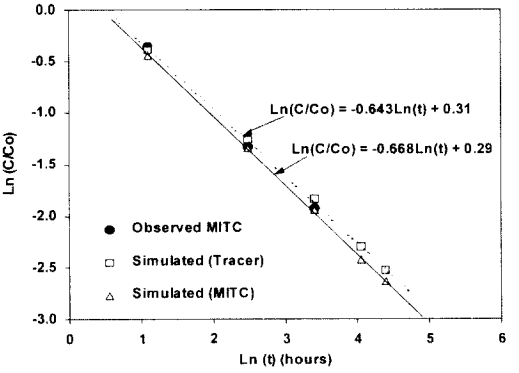

Figure 6. The linear relationships of observed and simulated MITC concentrations versus time during the early stage of the spill.

the observed MITC concentrations are quite lower than simulated values at stations 9 and 13.

Using natural log scales for time, Figure 6 compares the simulated tracer and MITC concentrations with the observed value versus time. The slopes obtained from the linear regressions of the tracer and MITC concentrations represent the dilution rate (q) and the combined rate of dilution and kinetic reactions (q + k), respectively. Thus, the difference (0.025 hr^{-1}) between q and q + k is the overall kinetic reaction rate (k) of MITC. The ratio of overall kinetic reaction rate to dilution rate (k/q) was about 4% along the various flow regimes, which agrees well with the results obtained in Table 2 (I_R = 0.9 - 6.9%).

Effect of Flow Regimes

The effect of reservoir flow regimes on the persistence of MITC during the late stage of the spill was quantified to examine the hypothesis that an interflow tend to delay the degradation of MITC and an overflow enhance it. An overflow regime was created by increasing the river water temperatures from 18-24 °C to 30 °C while all other conditions were unchanged. The spatial distributions of a conservative tracer (top) and MITC (bottom) concentrations for the two regimes are displayed in Figure 7, showing concentration contours 10 days after the peak concentration passed the inflow boundary.

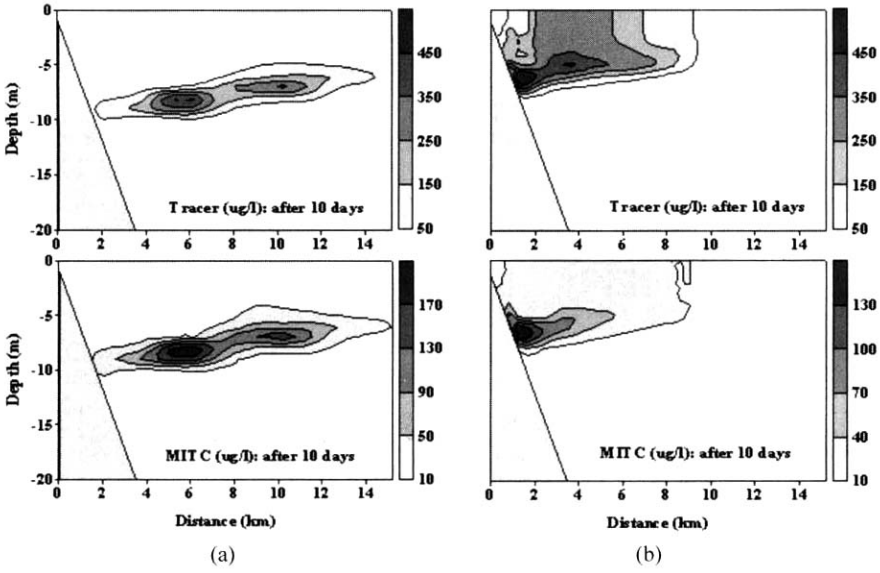

Figure 7. The spatial distributions of tracer (top) and MITC (bottom) concentrations in (a) the interflow and (b) overflow after 10 days (7/26/91).

In the interflow situation, the plume resided within the thermocline layer. The plume spread out in the longitudinal direction 6-10 m below the water surface while the head of plume reached up to 15 km from the upstream boundary. The peak concentrations are diluted to 350-450 μg/L due to mixing effect of flow only, which is indicated in the tracer concentrations. The combined effects of dilution and kinetic reactions resulted in further reduction of MITC concentrations to 130-200 μg/L. In the overflow case, the plume stayed near the surface of the reservoir and the plume head reached only up to 10 km from the upstream boundary. The peak concentration of tracer was about 350-450 μg/L, indicating that the level of dilution in the overflow situation is similar to that in the interflow. However, in the overflow, the toxic plume moved more slowly toward the dam and experienced greater degradation than the interflow did. This is due to the fact that the surface transport of the contaminant provided a suitable environment for great portion of MITC to be volatilized into the air. The concentrations were less than 60 μg/L in most part of the reservoir. These characteristics of an overflow regime may be considered as the positive aspects with respect to water quality management as drinking water intake and recreation facilities are generally located near the dam.

Figure 8 shows the maximum tracer and MITC concentrations versus longitudinal distance for the interflow and overflow situations. The concentration difference between tracer and MITC represents the amount of MITC decay. It is clearly shown that the effectiveness of physical and chemical reaction processes is greater in the overflow than in the interflow. The peak concentrations are reduced to 460 μg/L by flow dilution only in both flow regimes. In the interflow case, however, the MITC peak concentration (195 μg/L) was still greater than the LC_{50} for bluegill (130 μg/L). The peak concentration in the overflow was 107 μg/L, which is less than the LC_{50} for bluegill.

The effects of reservoir flow regime on the fate and transport of MITC are summarized in Table 3. Total reduction of MITC concentrations was mainly achieved by flow dilution (I_D > 95%) in the early stage of the spill, but the effectiveness of chemical reactions (E_R) increased with time as the turbulent mixing dimi-

Table 3. Effects of reservoir flow regime on the fate and transport of the toxic contaminant, MITC, in the late stage of the spill

Parameters	Flow regime	
	Interflow	Overflow
Propagation length (km)	15.0	10.0
Tracer concentrations (μg/L):		
Peak	460.0	460.0
Spatial average	210.0	220.0
MITC concentrations (μg/L):		
Peak	195.0	107.0
Spatial average	90.0	31.0
Reaction Index, I_R (%)	0.76	1.10
Effectiveness of reactions, E_R (%)	57.6	76.7

nished. After 10 days, the E_R values reached up to 57.6% and 76.7% for the interflow and overflow, respectively, indicating that the reduction of MITC is primarily attained through kinetic processes. Therefore, the persistence of the contaminant would be shorter if an overflow was created during the spill. An overflow may be the flow regime desirable for managing and remediation of a volatile toxic chemical in a reservoir during a spill.

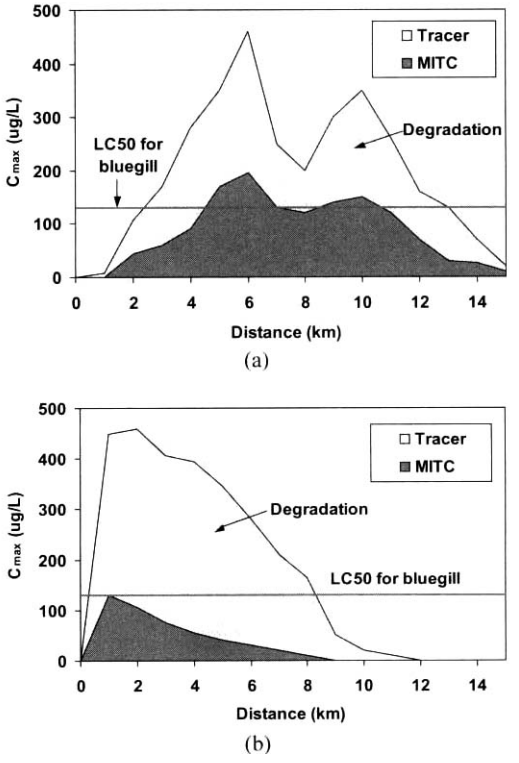

Figure 8. The longitudinal profiles of maximum tracer and MITC concentrations in the interflow (a) and overflow (b) regimes after 10 days.

CONCLUSIONS

A two-dimensional reservoir toxic module was developed and incorporated into the CE-QUAL-W2 model. The model is capable of simulating the fate and transport processes of toxic contaminants, including sorption and desorption, photolysis, hydrolysis, oxidation, biotransformation, volatilization, diffusive exchanges between the bottom sediment and water column, and sediment transport and deposition in a reservoir. The development of the toxic model enhanced the versatility of the original W2 model and provided an effective tool for describing and predicting the behavior of toxic contaminants in stratified reservoirs.

The model was applied to Shasta Reservoir, California to investigate the effect of various flow regimes on the fate of MITC that was spilled into the reservoir. Predicted temporal and spatial distribution of MITC concentrations clearly identified various reservoir flow regimes occurred during the spill, including plunge flow, underflow, and interflow that observed. Comparisons between the observed and predicted MITC concentrations showed that the model would be reliable for simulating the fate of MITC in the

reservoir. Results showed that the kinetic decay processes of MITC were slow in the interflow regimes, and that resulted in a long persistence of the chemical during the spill. In the early stage of the spill, MITC concentrations were mainly reduced by flow dilution due to transport and mixing processes, whereas, the effectiveness of kinetic processes for the chemical reduction increased with time as the turbulent mixing diminished in the late stage of the spill.

This study demonstrated that reservoir flow regime can substantially affect the persistence and transport of the volatile toxic contaminant in the late stage of the spill. The dilution levels in the interflow and overflow regimes were similar, while the overflow plume moved more slowly and experienced greater chemical loss. The overflow regime resulted in a reduced toxic contamination level (less persistent), shorter plume length, and longer response time compared to the interflow. These differences may be considered in water quality management as water intake structures and fishery facilities or other recreational activities are mostly located downstream near the dam. The model developed and results obtained in this study can be used to assist in spill control, field sampling and contamination remediation, and reservoir management including closure of water intakes.

ACKNOWLEDGEMENT

This work was supported by Chungbuk National University Grant in 2004.

REFERENCES

1. Capel, P. D., Giger, W., Reichert, P., and Wanner, O. "Accidental Input of Pesticides into the Rhine River," *Environ. Sci. Technol.*, **22**(9), pp. 992-997 (1988).
2. Chatterjee, P., California Suffers its Worst Chemical Spill., *New Scientist* 10 Aug., p. 12 (1991).
3. Goolsby, D. A., Battaglin, W. A., Fallon, J. D., Aga, D. S., Kolpin, D. W., and Thurman, E. M., "Persistence of Herbicides in Selected Reservoirs in the Midwestern United States: Some Preliminary Results," in *Selected Papers on Agricultural Chemicals in Water Resources of the Midcontinental United States.*, US Geological Survey. Denver, CO, USA (1993).
4. Eldridge J. C., Tennant, M. K., Wetzel, L. T., Breckenridge, C. B., and Stevens, J. T., "Factors Affecting Mammary Tumor Incidence in Chlorotriazine-treated Female Rats: hormonal properties, dosage, and animal strain," *Environ. Health Perspectives*, 102 (suppl. 11), pp. 29-36 (1994).
5. Munger, R., Isacson, P., Hu, S., Burns, T., Hanson, J., Lynch, C. F., Cherryholmes, K., Van Dorpe, P., and Hausler, Jr. W. J., "Intrauterine Growth Retardation in Iowa Communities with Herbicide-Contaminated Drinking Water Supplies," *Environ. Health Perspectives* **105**(3), pp. 308-314 (1997).
6. Chung, S. W. and Gu, R., "Two-dimensional Simulations of Contaminant Currents in a Stratified Reservoir," *J. Hydr. Engrg.*, ASCE. **124**(7), pp. 704-711 (1998).
7. Cole, T. M. and Buchak, E. M., CE-QUAL-W2: A Two-dimensional, Laterally Averaged, Hydrodynamic and Water Quality Model, Version 2.0 User Manual. Army Engineer Waterways Experiment Station, Vicksburg, Miss., USA (1994).
8. Martin, J. L., Application of two-dimensional water quality model. *J. of Environ. Engrg.*, ASCE **114**(2), 317-336 (1988).
9. Bath, A. J. and Timm, T. D., Hydrodynamic simulation of water quality in reservoirs of South Africa., *Commission Internationale Des Grands Barrages.*, Q.69 R. 39, 625-633 (1994).
10. Kim, Y. H, Kim, B. C., Choi, K. S., Seo, D. I., "Modeling of Thermal Stratification and Transport of Density Flow in Soyang Reservoir Using the 2-D Hydrodynamic Water Quality Model, CE-QUAL-W2," J. of the *Korean Society of Water and Wastwater*, **15**(1), pp. 40-49 (2001).

11. Park, O. R. and Park, S. S., "A Time Variable Modelling Study of Vertical Temperature Profiles in the Okjung Lake," *Korean J. Limnol.*, **35**(2), pp. 79~91 (2002).
12. Na, E. H., Ahn, K. H., Park, S. S., "A Modeling Study of Seasonal Overturn and Vertical Thermal Profiles in the Paldang Lake," *J. of Korean Society of Envir. Engr.*, **24**(5), pp. 901-910 (2002).
13. Schnoor, J. L, Environmental Modeling: Fate and Transport of Pollutants in Water, Air, and Soil, John Wiley & Sons, New York, USA (1996).
14. Lyman, W. J., Reehl, W. F., and Rosenblatt, D. H., Handbook of chemical property estimation methods, *McGraw-Hill*, New York, USA (1982).
15. Schnoor, J. L., Sato, C., McKechnie, D., and Sahoo, D., Processes, Coefficients, and Models for Simulating Toxic Organics and Heavy Metals in Surface Waters. EPA/600/3-87/015, Athens, GA, USA (1987).
16. Di Toro, D. M., "A Particle Interaction Model of Reversible Organic Chemical Sorption," *Chemosphere*, **14**(10), pp. 1503-1538 (1985).
17. Bierman, V. J. Jr., "Partitioning of Organic Chemicals in Sediments: Estimation of Interstitial Concentrations Using Organism Body Burdens," *Transport and Transformation of Contaminants Near the Sediment-Water Interface*, DePinto, J. V., Lick, W., and Paul, J. F. (Eds.), Lewis Publishers, Ann Arbor, pp. 153-175 (1994).
18. Di Toro, D. M., O'Connor, D. J., Thomann, R. V., and John, J. P., "Analysis of Fate of Chemicals in Receiving Waters, Phase I," *Chemical Manufact. Assoc.*, Washington, D.C., USA (1981).
19. Thomann, R. V. and Mueller, J. A., Principles of Surface Water Quality Modeling and Control, Harper & Row, New York, USA (1987).
20. Mackay, D., Volatilization of Organic Pollutants from Water. EPA/600/3-82/019, Athens, GA, USA (1982).
21. O'Connor, D. J., "Wind Effects on Gas-liquid Transfer Coefficients," *J. of Environ. Engrg.*, **109**(9), pp. 731-752 (1983).
22. Leonard, B. P., "A Stable and Accurate Convective Modeling Procedure Based On Quadratic Upstream Interpolation," *Computer Methods in Applied Mechanics and Engineering* **23**, pp. 59-98 (1979).
23. Rosario, A., Remoy, J., Soliman, V., Dhaliwal, J., Dhoot, J. and Perera, K, "Monitoring for Selected Degradation Products Following a Spill of VAPAM into the Sacramento River," *J. Environ. Qual.*, **23**, pp. 279-286 (1994).
24. Gu, R., McCutcheon, S. C., and Wang, P., "Modeling Reservoir Density Underflow and Interflow from a Chemical Spill," *Water Resources Research*, **32**(3), pp. 695-705 (1996).
25. Wang, P. F., Mill, T., Martin, J. L., and Wool, T. A., Fate and Transport of Metham Spill in Sacramento River," *J. of Environ. Engrg.*, **123**(7), pp. 704-712 (1997).
26. Worthing, C. R., The Pesticide Manual. 8th ed., The British Crop Protection Council, UK (1987).
27. Chung, S. W., Simulation and Analysis of Density Flows and Contaminant Transport in a Stratified Reservoir, M.S. Thesis, Dept. of Civil and Construction Engrg., Iowa State Univ., Ames, Iowa, USA (1996).
28. Tomlin, C., The Pesticide Manual. Tenth Edition, The British Crop Protection Council, UK (1994).
29. Zepp, R. G. and Cline, D. M., "Rates of Direct Photolysis in Aquatic Environment," *Eviron. Sci. Technol.*, **11**(4), pp. 359-366 (1977).
30. Draper, W. M. and Wakeham, D. E., "Rate Constants for Metam-sodium Cleavage and Photodecomposition in Water," *J. Agric. Food Chem.*, **41**, pp. 1129-1133 (1993).